

**Pre-print of:**

I. Lenton, et al., Orientation of swimming cells with annular beam optical tweezers, Optics Communications, 2019, 124864, ISSN 0030-4018, <https://doi.org/10.1016/j.optcom.2019.124864>.

© 2019. This manuscript version is made available under the CC-BY-NC-ND 4.0

license <http://creativecommons.org/licenses/by-nc-nd/4.0/>.

# Orientation of Swimming Cells with Annular Beam Optical Tweezers

Isaac C. D. Lenton\*, Declan J. Armstrong, Alexander B. Stilgoe, Timo A. Nieminen and Halina Rubinsztein-Dunlop

School of Mathematics and Physics, The University of Queensland, Brisbane, Queensland 4072, Australia

## ARTICLE INFO

### Keywords:

optical trapping  
dual beam trap  
annular beams  
spatial light modulator  
dynamic orientation  
motile particles

## ABSTRACT

Optical tweezers are a versatile tool that can be used to manipulate small particles including both motile and non-motile bacteria and cells. The orientation of a non-spherical particle within a beam depends on the shape of the particle and the shape of the light field. By using multiple beams, sculpted light fields or dynamically changing beams, it is possible to control the orientation of certain particles. In this paper we discuss the orientation of the rod-shaped bacteria *Escherichia coli* (*E. coli*) using dynamically shifting annular beam optical tweezers. We begin with examples of different beams used for the orientation of rod-shaped particles. We discuss the differences between orientation of motile and non-motile particles, and explore annular beams and the circumstances when they may be beneficial for manipulation of non-spherical particles or cells. Using simulations we map out the trajectory the *E. coli* takes. Estimating the trap stiffness along the trajectory gives us an insight into how stable an intermediate rotation is with respect to the desired orientation. Using this method, we predict and experimentally verify the change in the orientation of motile *E. coli* from vertical to near-horizontal with only one intermediate step. The method is not specific to exploring the orientation of particles and could be easily extended to quantify the stability of an arbitrary particle trajectory.

## 1. Introduction

In 2018 half of the Nobel prize in physics was awarded to Arthur Ashkin for the invention of optical tweezers (Ashkin, Dziedzic, Bjorkholm and Chu, 1986) and their application to the study of biological systems. Optical tweezers consist of one or more laser beams which can be used to apply pico-newton scale forces to small particles in order to trap them in three dimensions. Since the demonstration of three dimensional trapping by Ashkin in 1986 and a first demonstration of using it in biological systems in 1987 (Ashkin and Dziedzic, 1987), optical tweezers have been studied in numerous research labs around the world and used for broad studies of biological systems, reaching on one hand single molecule detection (Lang, Fordyce, Engh, Neuman and Block, 2004) and on the other hand trapping of very large objects deep in living tissue (Favre-Bulle, Stilgoe, Rubinsztein-Dunlop and Scott, 2017). Optical tweezers can be used to trap spherical particles, as well as a range of non-spherical particles, either in a single beam or with multiple beams to orientate the particle in a desired direction.

One example of a non-spherical particle that we are interested in is the rod-shaped bacteria *Escherichia coli* (*E. coli*) (Berg, 2004). This bacteria is of interest as a model organism which can be used to study, amongst other things, micro-scale fluid flow and swimming near surfaces. Using optical tweezers it is possible to hold motile *E. coli* by balancing the

\*Corresponding author

✉ [uqilento@uq.edu.au](mailto:uqilento@uq.edu.au) (I.C.D. Lenton); [declan.armstrong@uq.net.au](mailto:declan.armstrong@uq.net.au) (D.J. Armstrong); [stilgoe@physics.uq.edu.au](mailto:stilgoe@physics.uq.edu.au) (A.B. Stilgoe); [timo@physics.uq.edu.au](mailto:timo@physics.uq.edu.au) (T.A. Nieminen); [halina@physics.uq.edu.au](mailto:halina@physics.uq.edu.au) (H. Rubinsztein-Dunlop)

ORCID(s): 0000-0002-5010-6984 (I.C.D. Lenton); 0000-0001-6602-9832 (D.J. Armstrong); 0000-0002-9299-5695 (A.B. Stilgoe); 0000-0003-3055-7275 (T.A. Nieminen); 0000-0002-8332-2309 (H. Rubinsztein-Dunlop)

motility force with an equal but opposing force from the optical tweezers. By measuring the scattered optical tweezers beam, it is possible to get an accurate measurement for the swimming force (Bui, Kashchuk, Balanant, Nieminen, Rubinsztein-Dunlop and Stilgoe, 2018). Further, by tracking the particle's position, it is possible to simultaneously measure the velocity enabling studies of the relationship between swimming velocity and swimming force. In order to facilitate these studies, we need to be able to manipulate *E. coli* in order to orientate the particle in a desired direction.

Some cells can be directly manipulated using holographic optical tweezers (HOT). For example, Hörner, Woerdemann, Müller, Maier and Denz (2010) trap and orientate multiple *Bacillus subtilis* (a 3  $\mu\text{m}$  bacterium similar to *E. coli*) simultaneously using HOT with two traps, one at each end of the bacterium. The traps can be gradually moved in order to rotate the particle or change the particle's position. In another experiment, Carmon and Feingold (2011) rapidly scan a single beam between the two end points of the bacterium. The advantage of scanning the beam in this way avoids interference between the optical traps, allowing for tighter confinement in the axial direction. Particles can also be aligned using structured light fields or other more specialised approaches. For example, optical tweezers formed at the tip of an optical fibre have been used to create structured light fields for orientating *E. coli* (Huang, Liu, Zhang and Li, 2015). HOT can be used to manipulate several particles at once or rotate larger structures such as micro-rotors, which in turn can be used to generate fluid flows for indirectly manipulating particles (Bütaitė, Gibson, Ho, Taverne, Taylor and Phillips, 2019).

Our present goal is to align motile *E. coli* perpendicular to the beam axis to enable us to study how these cells behave in certain environments. Although *E. coli* and similar rod-shaped bacteria have been previously orientated using scanned beams and HOT (Hörner et al., 2010; Carmon and Feingold, 2011), we found it can be difficult to reproduce these results using our existing experimental setup. Factors such as the numerical aperture, aberration or greater motility of the bacteria compared to these previous studies make the experiment difficult to perform. We previously had success orientating several-days old *E. coli* (unhealthy, less motile) using HOT and line shaped traps. We were unable to reproduce the results with healthier and more motile *E. coli*. We also explored using other shaped beams including tug-of-war tweezers, which have been demonstrated for stretching elongated cells (Lamstein, Bezryadina, Preece, Chen and Chen, 2017). While some of these approaches worked in simulations, it can be difficult to realise these traps in a lab experiment. Aberrations and an insufficient numerical aperture can reduce the trapping effectiveness of intricate structured light fields.

In this work, we describe the use of annular beams to hold *E. coli* and dynamically change the potential in order to align the particle to a desired orientation. Annular beams have a simple structure which has been previously observed to reduce back reflection and thus can improve axial optical trap depth—one of the problems in our earlier experiments. We use a spatial light modulator to generate and dynamically change the position of the annular beams. Using simulations, we are able to explore the angular trap stiffness along the path the *E. coli* takes when we shift the beams. We investigate the number of intermediate patterns required to change the *E. coli* orientation from vertical to horizontal in order to increase the transition speed on devices with a finite frame rate. Our method is simple and robust since it only requires a device capable of displaying a few discrete patterns and doesn't depend on specialised high speed devices. The paper is split into two main parts: a background section which provides an overview of optical trapping and the generation of annular beams, and a results section which describes our investigations targeted at orientation of motile *E. coli*.

## 2. Background

The principal behind optical tweezers is the transfer of momentum from one or more laser beams to a particle. Scattering and absorption by the particle leads to a change in the laser beams momentum, resulting in a corresponding force on the particle. The force transferred to the particle depends on the beam power, the amount of scattering and the speed of light in the medium. The amount of scattering in-turn depends on the particle size and shape, the relative refractive index of the particle in the surrounding medium, as well as the overlap between the beam (shape) and the particle (shape). The optical force is often separated into two components: the gradient force and the scattering force. The gradient force is proportional to the gradient of the electric field and is either attractive or repulsive depending on the refractive index of the particle relative to the surrounding medium. Particles with a refractive index greater than the surrounding medium will be attracted by the gradient force towards more intense regions of the beam, while particles with a lower refractive index will be repelled. The scattering force arises from light reflected or absorbed by the particle, and often acts to push the particle along the beam axis. For particles with a higher refractive index than the surrounding medium, stable trapping in three dimensions requires overcoming the scattering force. This can

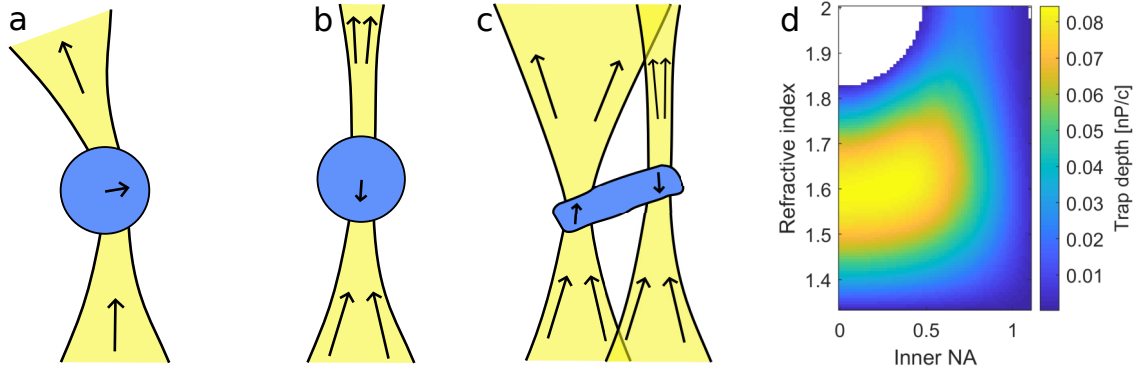


**Figure 1:** (a–c) Illustrations showing the optical force on dielectric particles due to the transfer of momentum from the light beam to the particle. (a) and (b) show optical forces on a spherical particle trapped in a Gaussian-like beam. (c) shows an elongated particle in a dual beam optical trap. (d) demonstration of how annular beams can be used to improve trap depth for trapping of a spherical particle (radius  $R \approx 0.46\lambda_0$ ) in water (refractive index  $n = 1.33$ ). As light is removed from the centre of the beam (Inner NA  $\rightarrow 1$ ), the range of particles which can be trapped increases.

be achieved, for instance, by using counter-propagating beams (Ashkin, 1970), balancing the scattering force with another force such as gravity (Ashkin and Dziedzic, 1971), or by using a tightly focused beam such that the gradient force overcomes the scattering force (Ashkin et al., 1986).

The simplest optical traps typically involve using a tightly focused laser beam, often a beam with a Gaussian profile, to trap and manipulate particles. For spherical particles trapped in a Gaussian beam, the gradient force typically results in the particle being trapped at the beam focus or, if the particle is strongly scattering, slightly downstream of the focus. A small dielectric particle can be thought of as a small lens. When the particle moves through the beam it will change the direction and collimation of the beam. The particle will experience a corresponding force, opposing the change in momentum of the beam, as illustrated in figure 1 (a–b) for a particle with a refractive index higher than the surrounding medium. The optical force can be increased by changing the refractive index contrast between the particle and medium, increasing the power, or by changing the beam phase/amplitude distribution. In some circumstances, increasing the refractive index contrast can improve trapping; however, the corresponding increase to the scattering force often leads to the particle no longer being stably trapped in three dimensions. By using structured light beams, such as annular beams, it is possible to reduce the scattering force and improve the trap quality.

Trap quality can be measured in a number of ways including trap stiffness, which is a measure of how steep the gradient is around the trap centre; and trap depth, a measure of how much force can be applied before the particle escapes. In this paper, we define the trap depth as the minimum of the peak restoring force/torque in a particular direction, i.e., the maximum force or torque that can be applied to the particle before it escapes the trap. The trap depth has the units of force. We use the dimensionless quantities  $nP/c$  and  $P/\omega$  for optical force and torque, where  $n$  is the refractive index of the medium,  $P$  is the beam power and  $c$  is the speed of light in vacuum. These quantities give the force in units of  $n\hbar k$  per photon and torque in units of  $\hbar$  per photon (Nieminen, Du Preez-Wilkinson, Stilgoe, Loke, Bui and Rubinsztein-Dunlop, 2014). Similar quantities can be defined for non-spherical particles in terms of the torque aligning the particle to a particular direction.

Figure 1 (d) shows how trap depth for a spherical particle in an annular beam changes as a function particle refractive index and beam shape (in this case the inner numerical aperture (NA) of the annular). Annular beams may refer to beams where the centre has been removed in the far-field, or the term may refer to a beam with a phase discontinuity at the centre, creating a doughnut shape in the near-field. In this paper we use the term annular beam to refer to beams where the central portion has been removed in the far-field. This type of annular beam can be described by two angles (numerical apertures) for the interior and exterior ring radii. For reflective or absorbing particles, annular beams can improve trapping by reducing the amount of light in the centre of the beam contributing to the scattering or absorption force (Ashkin, 1992; Padgett and Bowman, 2011). The top left corner of figure 1 (d) shows a region where a high contrast particle cannot be trapped. By using an annular beam, a range of particles with a much larger variety of refractive indices can be trapped and the trap depth is improved for certain refractive-index/beam combinations. The motivation for this current study was to understand if a similar improvements could be seen for the orientation of

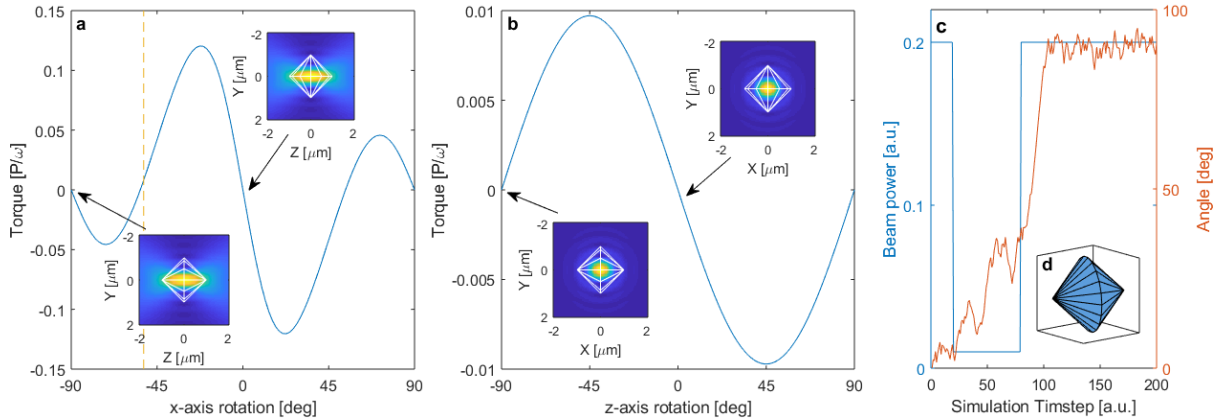


**Figure 2:** (a-b) torque-rotation plots for a particle (d) with multiple stable angular equilibria. The dashed line in (a) marks the unstable equilibrium between the two stable traps. Insets show particle orientation in the beam. (c) shows the beam power and the angle between the particle axis and beam axis from Movie 1. (d) shows the particle used in these simulations, a reminiscent of two cones stacked on top of each other.

rod-shaped particles perpendicular to the beam axis.

For non-spherical particles, it is often desirable to be able to control not just the position but also the orientation. Small elongated particles, such as *E. coli*, held in a Gaussian beam, tend to align either along the beam axis or along the polarisation axis, depending on the size and aspect ratio (Simpson and Hanna, 2011; Cao, Stilgoe, Chen, Nieminen and Rubinsztein-Dunlop, 2012). If the particle is sufficiently large, it may be possible to grab different parts of the particle with multiple traps, as illustrated in figure 1 (c). Or, it may be possible to use beam shaping to generate a light field which orientates the particle in the desired orientation. In any case, there are frequently multiple stable equilibria which the particle may become aligned to. For example, in the twin beam case shown in figure 1 (c), the particle could become aligned in either of the beams individually.

When the particle size approximately matches the size of the beam or features of the shaped beam, there are often multiple stable equilibria. Alignment of these particles can be achieved by switching between the different equilibria. For certain non-motile particles, such as certain crystals or bacteria spores, particles will naturally drift between different equilibria if the temperature is high enough or the trap power is low enough. Thus, it is possible to switch between equilibria by simply lowering the power of the laser, letting the particle diffuse through Brownian motion, and increasing the power once the desired orientation has been achieved; as shown for a crystal-like dielectric particle in Figure 2 and Movie 1. Movie 1 demonstrates this method for changing the orientation between two stable equilibria, separated by an unstable equilibrium at  $\sim 38^\circ$ . The beam power is lowered to allow the particle to rotate through Brownian motion. Once the particle has passed  $\sim 38^\circ$ , corresponding to the unstable equilibrium marked in Figure 2 (a), the trap power is raised and the particle falls into the new equilibrium. The positions of the stable and unstable equilibria, and the corresponding times when beam power must be raised/lowered, depend strongly on the particle size/shape.

Trapping of live cells including bacteria is more difficult. If the power is too high, cells can be damaged by absorption and subsequent heating (Zhang and Liu, 2008; Neuman and Block, 2004). In addition, many living cells are also motile, some moving at speeds of microns per second. If the power is too low, these particles tend to escape from the trap. This makes it difficult to move the particle between different equilibria using the previously described method, since lowering the power can lead to the particle rapidly swimming out and away from the trap. Furthermore, when trapped, motile particles are able to explore a greater range of the optical potential, often escaping traps that would hold similarly shaped non-motile particles. By using sculpted light beams, it is possible to create traps which strongly confine a particular shaped particle to a specific position and orientation. The orientation and position can be changed by dynamically changing between different shaped beams.

There are a number of methods for generating different shaped light fields including using multiple beams, modulating the phase or amplitude of a single beam, or rapidly scanning a single beam between multiple positions. Multiple traps can be generated using different lasers, beams with different polarisation, or with diffractive optical elements to

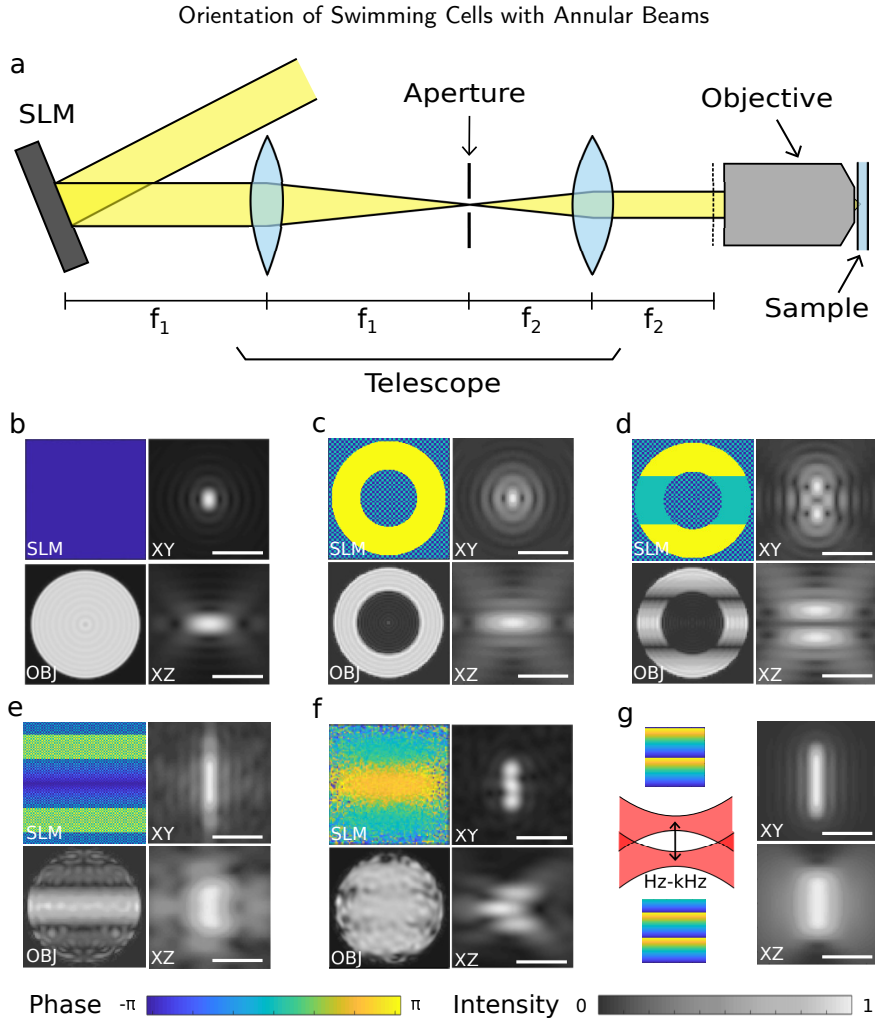


**Figure 3:** (a) overview of optical tweezers system including a spatial light modulator (SLM) for phase modulation. The aperture is used to remove light scattered to high angles.  $f_1$  and  $f_2$  are the focal lengths of the lenses forming the telescope. (b–g) simulations of different kinds of beams and the corresponding phase at the SLM plane: (b) uniform phase and illumination, (c) annular beam, (d) twin annular beam, (e) line trap generated using sinc pattern, (f) line trap generated using Gerchberg-Saxton algorithm, (g) line trap generated by scanning the beam. OBJ shows the light intensity at the objective back-focal plane, marked by the dotted line in (a). XZ and XY show the light near the focal plane, the scale bar shows  $\sim 2\mu\text{m}$ . All beams have linear polarisation. The aliasing effect in (c–e) SLM is an artefact of rendering the  $512 \times 512$  pixel checkerboard pattern at a lower resolution in the figure.

split the light between multiple traps. Devices such as the digital micro-mirror device or liquid crystal spatial light modulator (SLM) can be used to rapidly change the intensity or phase of the beam. These devices can be fast, with some devices operating at kHz speeds (Gauthier, Lenton, Parry, Baker, Davis, Rubinsztein-Dunlop and Neely, 2016; Stuart and Kuhn, 2018); they can be used to create multiple holographic optical tweezers (HOT) for manipulating multiple particles simultaneously (Dholakia and Čižmár, 2011; Padgett and Bowman, 2011); and they can also be used to change the shape of the beam in order to better match the shape of the particle and improve trap stiffness/depth (Woerdemann, Alpmann, Esseling and Denz, 2013; Roichman and Grier, 2006). In this paper we use a phase-only SLM to modulate the incident beam. The SLM is imaged onto the back focal plane of the microscope objective, as shown in figure 3 (a). A telescope can be used to reduce or enlarge the beam in order to fill (or over/under-fill) the microscope back aperture. An aperture between the telescope lenses allows additional spatial filtering of the beam, this can be useful for achieving amplitude control with a phase-only device.

Figure 3 (b–g) shows different kinds of beams simulated using the optical tweezers toolbox (OTT) (Nieminen,



Loke, Stilgoe, Knöner, Brańczyk, Heckenberg and Rubinsztein-Dunlop, 2007; Lenton, Stilgoe, Nieminen, Loke, Hu, Knöner, Branczyk, Heckenberg and Rubinsztein-Dunlop, 2019). Optical tweezers systems typically use high NA objectives and the resulting focused fields are non-paraxial. In order to simulate the focused fields and calculate the optical forces/torques we used the point matching method to match the paraxial far-field to the vector spherical wavefunction expansion in the far-field (Nieminen, Rubinsztein-Dunlop and Heckenberg, 2003). We simulated a water immersion objective (NA=1.2) and assumed a  $\sin \theta$  mapping between SLM pixel coordinates and focusing angle. Figure 3 (b) shows a beam with uniform phase and uniform amplitude at the back aperture of the objective. This beam can be converted into an annular beam by simply removing the central portion of the beam, as shown in figure 3 (c). An elongated particle will align in these beams either along the beam axis or along the polarisation axis, depending on size/shape.

Our present interest is in orientating *E. coli*. In order to do this, we have investigated a number of different kinds of beams. Figure 3 (d–g) show different kinds of beams intended to align rod-shaped particles perpendicular to the beam axis. The simplest configuration is dual beam optical tweezers, which have previously been demonstrated for trapping *E. coli* (Hörner et al., 2010). These can be generated by simply superimposing the diffraction pattern for each beam (a linear phase grating controlling the position of each beam). Figure 3 (d) shows dual annular beam optical tweezers, the phase pattern is simply the dual beam optical tweezers phase pattern with the centre removed. We also explored the stripe (or line) beam (Roichman and Grier, 2006), shown in figure 3 (e). Non-motile particles would align to the beam but motile particles would swim out the ends of the beam. We assumed this was because of the weaker trap strength along the line. Figure 3 (f) shows a beam generated using the Gerchberg-Saxton algorithm (Gerchberg and A Saxton W., 1971). The beam has sharp features in the XY plane, however the axial intensity shows large lobes. In simulations, we found motile *E. coli* tend to align vertically in these kinds of lobes and don't trap in the desired orientation. Figure 3 (g) shows a scanned beam. These beams have been previously shown to be able to hold *E. coli* (Carmon and Feingold, 2011) however our current experimental system doesn't support creating beams with this method.

Simulations suggested that the dual (annular) beams should hold *E. coli* horizontally, however our initial efforts at orientating *E. coli* with these beams were unsuccessful. When we simulated particles swimming into the trap, we found that they would tend to align in a single beam and not reach the centre of the trap. In the following section we discuss the use of annular beams and dynamically changing the SLM pattern for the orientation of *E. coli*.

### 3. Orientation of motile *E. coli*

This section is split into three parts: generation of dual annular beam optical tweezers using an SLM, orientation of motile *E. coli* using dynamic potentials and an overview of a method for characterising the *E. coli* trajectory.

#### 3.1. Generation and Control of Annular Beams

Annular beams are characterised by a distinctive darkened patch in their centre far from a focus and can be created in a number of ways including using a SLM (see figure 3 (c–d)), with a fixed mask (Oliveira, Campos and Rocha, 2018; Dear, Burnham, Summers, McGloin and Ritchie, 2012), or with a pair of axicons (Lei, Li, Yan, Yao, Dan, Qi, Qian, Yang, Gao and Ye, 2013). In this section we investigate the use of annular beams on rod-shaped particles to determine if there is a similar improvement for angular trap stiffness.

We use a computer controlled SLM to create the annular beams used in the experiments. We control the annular beam position by applying a linear phase function for transverse displacement and a parabolic phase function for axial displacement,

$$\phi_{\text{lens}}(x, y) = \frac{x^2 + y^2}{2R} \quad (1)$$

$$\phi_{\text{linear}}(x, y) = Dx \quad (2)$$

where  $D$  and  $R$  control the magnitude of displacement for the beam. To rotate the *E. coli*, we combine the phase patterns for each beam using

$$\phi_{\text{twinn}} = \arg \left\{ e^{i\phi_{\text{linear}} \sin \theta + i\phi_{\text{lens}} \cos \theta} + e^{-i\phi_{\text{linear}} \sin \theta - i\phi_{\text{lens}} \cos \theta} \right\} \quad (3)$$

this produces a double spot pattern with elliptical (circular for calibrated  $D$  and  $R$ ) trajectory as a function of angle  $\theta$ . The choice of  $D$  and  $R$  affects the trap stiffness along the particle axis; these parameters can be adjusted to give good trap stiffness in the vertical and horizontal particle orientations.

An annular beam is generated by removing the inner central portion of a Gaussian or flat-top beam. With a amplitude-type SLM, such as a digital micro-mirror device, the required mask can be generated by simply setting the output in the central region to zero. We use a phase-only SLM, which can not directly control the beam amplitude. Instead, we introduce a second pattern to scatter light to other locations in the far-field. We use a checkerboard pattern to scatter light to large angles outside our optical path (Wong and Chen, 2008; Stilgoe, Kashchuk, Preece and Rubinsztein-Dunlop, 2016). A iris or aperture can be used to remove this light, as shown in figure 3 (a). The resulting pattern is

$$\phi_{\text{annular}}(x, y) = \begin{cases} \phi_{\text{twin}} & r_1 < \sqrt{x^2 + y^2} < r_2 \\ \phi_{\text{checker}} & \text{otherwise} \end{cases} \quad (4)$$

where  $r_1$  and  $r_2$  are the inner and outer radius of the annular beam. In our experiments we set  $r_2$  to approximately the same size as the radius of the objective back aperture. To implement these functions and control the SLM we use our soon-to-be released beam shaping toolbox, OTSLM. An example phase pattern and simulated far-field for one of these double-spot annular beams is shown in figure 3 (d).

To understand effect of using these beams on the angular trap depth, we used the optical tweezers toolbox to simulate the beams (Nieminen et al., 2007; Lenton et al., 2019). We choose to explore how changing the inner radius of the annular beam while keeping the beam power fixed affects the trap depth. Figure 4 shows the angular trap depth for rod-shaped particles in twin annular beams with and without spherical aberration. We first determined if the particles could be trapped and if the particle could be orientated horizontally between the two annular beams. For rod-shaped particles in the twin annular beams, we observed very little change for low refractive indexes like *E. coli* in water; in some cases the trap depth was reduced by using annular beams.

By using annular beams, there is an improvement to the range of high index particles which can be trapped, this would be useful, for instance, trapping rod-shaped micro-organisms or spores in air or vacuum. When certain spherical aberrations are added to the beams, both the range of particles that can be trapped and the trap depth are significantly reduced for non-annular beams but appear to improve for annular beams. Investigating how these beams look with spherical aberration, we see how the annular beams maintain their general shape for small deviations, while Gaussian-like beams become more elongated in the axial direction (figures 4 (b–c, e–f)). In some cases, these spherical aberrations may enhance trap stiffness or create additional trapping equilibria (Stilgoe, Heckenberg, Nieminen and Rubinsztein-Dunlop, 2011). While annular beams may not provide an improvement in general, it is important to consider the size of the annular beam as well as the direction of the spherical aberration.

These results, although interesting, are not particular useful for trapping of *E. coli* in water. In systems with strong spherical aberrations, it is often possible to correct for the aberration using an SLM or phase mask (Itoh, Matsumoto and Inoue, 2009; Wulff, Cole, Clark, DiLeonardo, Leach, Cooper, Gibson and Padgett, 2006). However, using an annular beam can be simpler than implementing one of these methods. Annular beams would be more suitable for trapping of high contrast particles, such as trapping cells in air or vacuum (Pan, Berg, Zhang, Noh, Cao, Chang and Videen, 2011).

### 3.2. Orientating Motile *E. coli* with Dynamic Potentials

Our simulations showed that one of the difficulties with orientating motile *E. coli* was with loading them into the dual beam trap. The *E. coli* would often align with one of the annular beams rather than aligning between the two. This difficulty was encountered for both annular and Gaussian dual beam tweezers. Although rod-shaped bacteria have been previously orientated using this method (Hörner et al., 2010), we found it difficult to reproduce these results in our experiment using *E. coli*, perhaps due to increased motility or the shorter length of the bacteria. To orientate the *E. coli* more reliably, we found it better to start with the *E. coli* aligned to the beam axis before attempting to change the orientation. By gradually changing the SLM pattern, we were able to orientate the particles in the desired direction.

In our experiment, we trap motile *E. coli* using HOT; the setup has been previously described in (Kashchuk, Nieminen, Rubinsztein-Dunlop and Stilgoe, 2019), and here we only give a brief summary. We use a 1064 nm fiber laser (YLR-10-1064-LP, 10W, IPG Photonics) focused by a high numerical aperture objective (Olympus UPlanSApo 60×, water immersion, 1.2 NA). For beam shaping, we use an SLM (Meadowlark Optics, 512x512 HSP512L, high-speed SLM) imaged onto the back focal plane of the objective (as shown in figure 3). The *E. coli* is trapped in a buffer solution (consisting of potassium phosphate, EDTA and KCl), with a refractive index similar to water, between two microscope coverslips spaced with double-sided tape ( $\sim 0.1$ – $0.2$ mm thick).

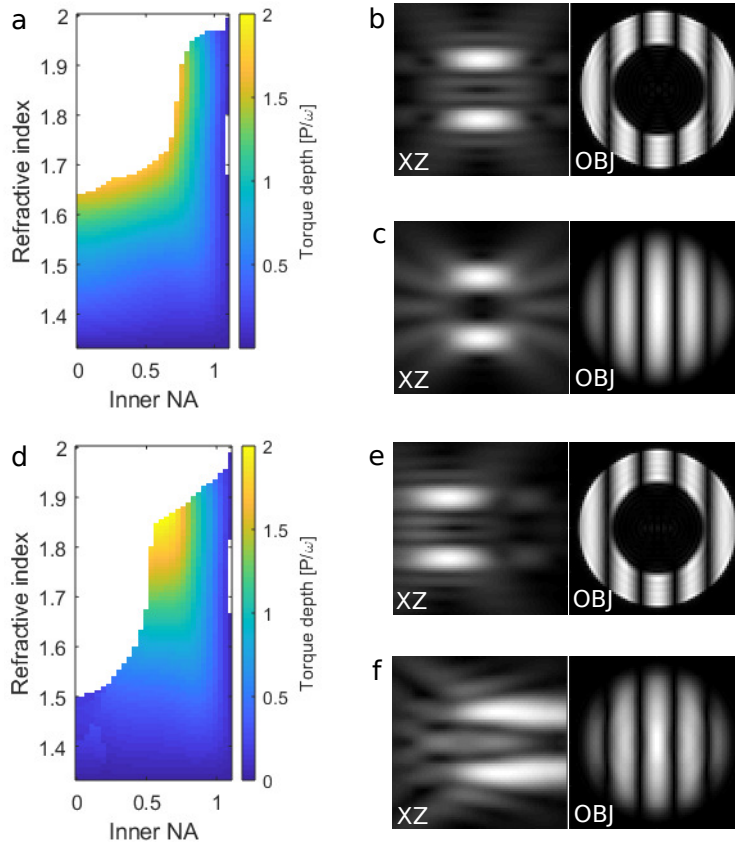


**Figure 4:** Exploration using dual annular beam optical tweezers (separation  $1.8\mu\text{m}$ ) to trap a rod-shaped particle (length  $3\mu\text{m}$ , radius  $0.5\mu\text{m}$ ) horizontally. (a) angular trap depth for rod-shaped particle, (b–c) annular and Gaussian beam near-field (XZ) and far-field (OBJ) intensity. (d–f) show how the previous results change with the introduction of a spherical aberration.

We started with the *E. coli* trapped in a single beam and then displayed a sequence of patterns to gradually move the traps from both being aligned with the beam axis to both being separated transverse to the beam axis. To trap the *E. coli*, we tried different parameters controlling the inner annular radius, linear grating periodicity and lens grating spacing. The separation of the two traps (i.e., the linear and spherical grating parameters) were roughly determined by the length of the particle, as previously noted by (Català, Marsà, Montes-Usategui, Farré and Martín-Badosa, 2017). To measure the quality of the trap, we used measurements of the force in the direction of trap separation to determine trap stiffness. Figure 5 (a) shows results for different inner radius of the annular beam; the incident power on the SLM was held fixed. Trap stiffness was determined from the corner frequency in the power spectral density of the force measurements. As the inner radius was increased, the trap stiffness decreased. The most significant contribution to the decrease in trap stiffness was the decrease in beam power as more light was removed from the centre of the beam. However, this alone doesn't account for the observed behaviour. For the motile *E. coli* used in the experiment, the change in equilibrium position due to the swimming force must also be considered. When the beam power changes, the ratio of optical force to swimming force changes, causing the equilibrium position to change. The optical force curves are highly non-linear, as shown in figure 5 (b); and small changes to the equilibrium position can have huge changes on the measured trap stiffness. Using simulations, we were able to explore the effect of different ratios of swimming force to optical force, producing the shaded region shown in figure 5 (a).

We also used simulations to explore the effect of trap separation on optical force and particle orientation. Figure 5 (b–c) show the optical force and orientations for three different beam configurations: two Gaussian-like beams and an annular beam. The simulations show that the choice of trap separation as a ratio of particle length has a significantly greater impact on trap properties than the choice between Gaussian or annular beams for low index rod-shaped



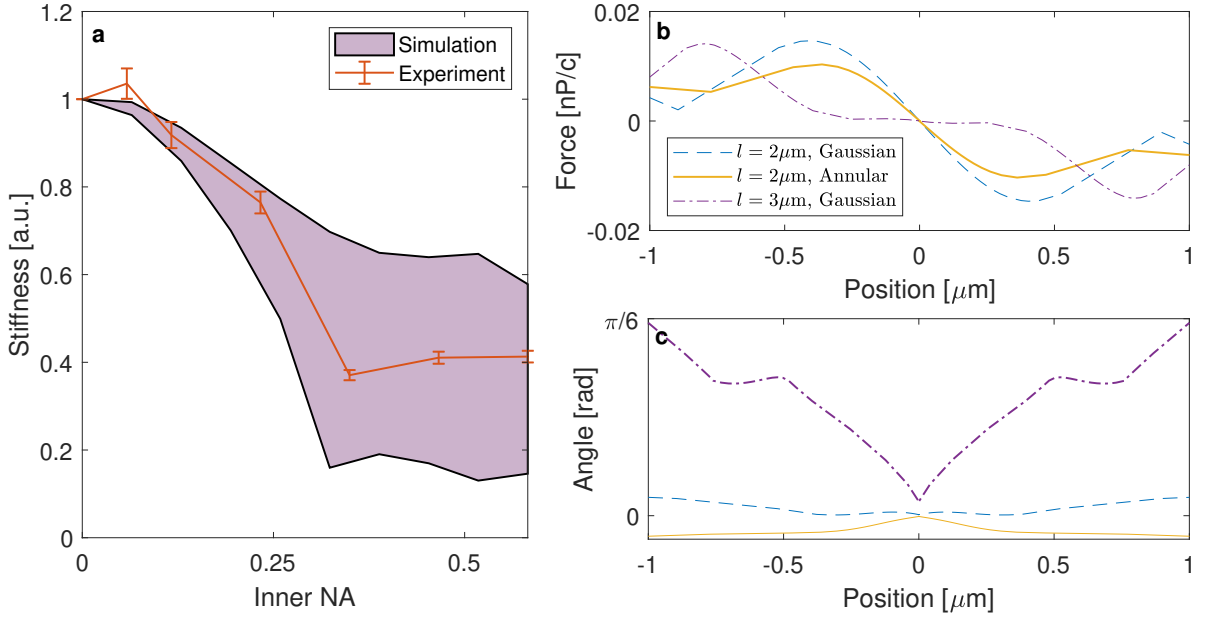


**Figure 5:** Exploration of trap properties for *E. coli* in twin annular beams. (a) shows numerical modelling and experimental measurements of the trap stiffness in the direction of trap separation for motile *E. coli* as a function of inner beam radius for fixed SLM illumination. The shaded region shows the range of predicted trap stiffness for different ratios of the trap power and *E. coli* motility force. Approximate values for the *E. coli* shape (length  $l = 2\mu\text{m}$  and radius  $r = 0.5\mu\text{m}$ ) and refractive index ( $n = 1.36$ ) were used for numerical simulations. (b) Simulation of the measured force for Gaussian-like (Inner NA = 0) and Annular (Inner NA = 0.58) beams with different *E. coli* lengths ( $l$ ). (c) angle of *E. coli* relative to the plane transverse to the beam axis for the beams in (b).

particles in water. A mismatch between the particle length and trap separation leads to a lower stiffness between the force maxima, as previously observed by Català et al. (2017) for cylinders in multiple traps or Meissner, Oliver and Denz (2018) for elongated particles in a single trap. The observed trap stiffness for a particle in such a trap will strongly depend on the particle's motility. If the particle is non-motile, the equilibrium position will be around the centre of the force maximum and the stiffness will be approximately 0. However, for motile particles, the equilibrium position will be closer to one of the maxima (depending on the swimming direction) and the stiffness will be significantly larger. For this reason, care must be taken when using trap stiffness measurements to quantify the optical trap quality of motile particles. Further, if the spacing between the two traps was too small, particles may not sit horizontally, as shown in figure 5 (c). For systems without axial force detection, accurate motility force (and stiffness) measurements require precise orientation or accurate estimates for the misalignment.

### 3.3. Achieving Fast Orientation using Discrete Potentials

Using the SLM we were able to gradually change the position of the two annular beams. We would like to determine how fast we can change between patterns and how many intermediate patterns we need in order to change the orientation of the particle. To determine this, we simulated a motile *E. coli* shaped particle. We assumed the particle swims in one direction with a constant swimming force. To quantify the stability of a particular transition, we calculated the average trap stiffness over the time  $\Delta t$  it took the particle to make the transition in the direction of the desired equilibrium. This average is given by

$$\langle k \rangle = \frac{\int_0^{\Delta t} \vec{k} \cdot \vec{x} dt}{\Delta t} \quad (5)$$

where  $\vec{k}$  is the trap stiffness

$$\vec{k} = \frac{d\vec{F}}{d\vec{x}}, \quad (6)$$

and  $\vec{x}$  is a unit vector in the direction of the target equilibrium. This approach assumes that the particles trajectory doesn't vary significantly from the equilibrium trajectory when Brownian motion is included. If the particle remains trapped and only rotates, i.e., the position remains relatively unchanged throughout the trajectory, we can approximate the above integral by

$$\langle k \rangle \approx \frac{\int_0^{\Delta t} k_\theta dt}{\Delta t} \quad (7)$$

where  $k_\theta$  is the angular trap stiffness

$$k_\theta = \frac{d\tau_\theta}{d\theta} \quad (8)$$

for the torque  $\tau_\theta$  about the rotation axis  $\theta$ .

There are multiple sensible values for  $\Delta t$  including: the time required for the particle to reach an equilibrium orientation, a step size related to the update rate of the device displaying the pattern, or an arbitrary duration. If an arbitrarily long duration is chosen, this will bias  $\langle k \rangle$  towards transitions with high trap stiffness at the equilibrium position. This could be useful for designing trajectories with very stable intermediate positions. If instead the rate is equal to the time taken for the particle to come to equilibrium,  $\langle k \rangle$  will be less biased towards the stiffness at the equilibrium. In this case, subsequent transitions should be made as soon as the equilibrium is reached since information about stability at the equilibrium is not included in the estimate. Alternatively, if the particle re-orientates much faster than  $\Delta t$ , it should be possible to reformulate the above expressions in terms of the position traversed by the particle before it reaches equilibrium. The reformulation in terms of position only works for slowly varying fields. For rapidly varying fields, such as scanned beam optical traps (Carmon and Feingold, 2011), it is necessary to consider the different times scales of the particle motion, trap frequency and damping. Here we use the time formulation.

We choose a moderately long value for  $\Delta t$  so that the particle could come to equilibrium and be stably trapped after each transition. For a device, such as a liquid crystal based SLM, with a relatively slow finite update rate (compared to the particle rotation rate), it is important to have a stable trap position between each orientation step. To understand how different step sizes affect the particle orientation, we simulated the particle swimming in a low Reynolds number environment in the absence of Brownian motion (Volpe and Volpe, 2013). By calculating the trap stiffness towards the horizontal equilibrium, we were able to estimate the strength of the optical trap for different step sizes, given a particular starting angle. In our simulations, we observed that the ability to rotate the particle is affected most by the choice of the first few steps. As figure 6 (a) illustrates, it is very difficult to rotate the particle from vertical to horizontal with no intermediate steps, i.e., the particle either falls out of the trap or gets trapped aligned with the beam axis in one of the annular beams. With just one intermediate step, it is possible to bypass the initial low stiffness region and jump to a region where a subsequent step can correctly orientate the particle. To understand this behaviour, we plotted the average stiffness towards the equilibrium (Eq. 7) for a range of different starting positions and step sizes for our specific annular beam, see Appendix A. For large steps at small initial angles, the average trap stiffness is small or positive and the resulting angle after the step doesn't match the trajectory with small steps. We found the size of the positive stiffness region depends strongly on the beam properties and the particle shape. However, a consistent choice for rod shaped particles in Gaussian and annular beams seemed to be a relatively large initial step ( $\sim 0.15$ – $0.7$  radians) followed by one or more steps to bring the particle to the horizontal equilibrium.

Our simulations suggested it should be possible to orientate the particle from vertical to horizontal with one intermediate step. A simulated trajectory (both with and without Brownian motion) is shown in figure 6 b. When the trap positions are changed, there is a short period of time before the particle position stabilises. During this time, the particle also moves vertically/horizontally in the trap and in some cases this will cause the angle to initially jump up (as is the case around Time= 0s). When Brownian motion is included, the size of these jumps is noticeably reduced in the particle orientation plot, however the jumps are still observed in the particle position. To verify our results, we were able to demonstrate orientation experimentally, the insets in figure 6 b show images from the experiment. The final inset shows the particle aligned approximately horizontal, fluctuations in the particle angle are likely caused by

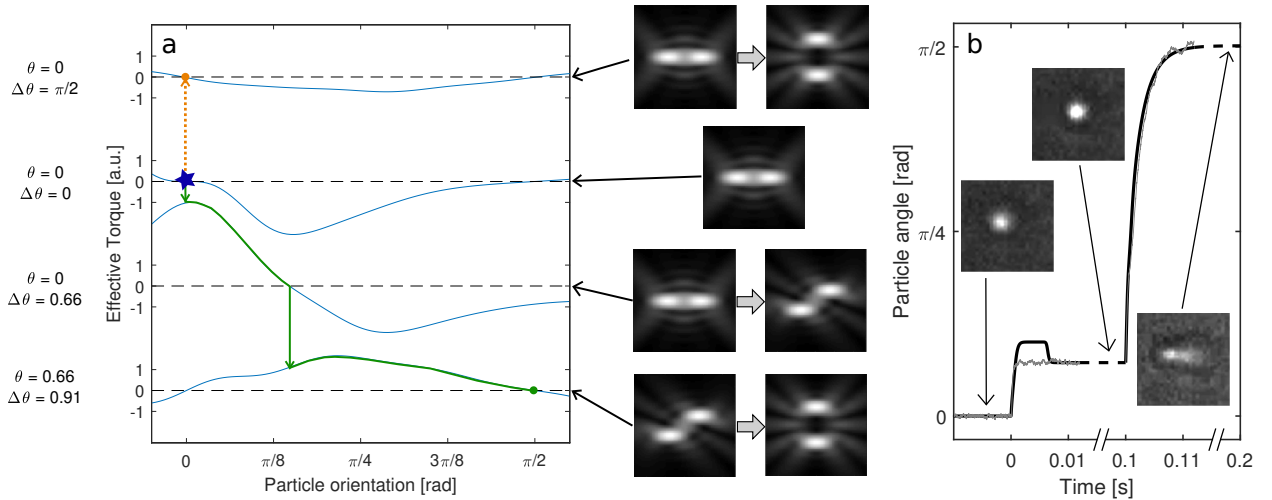


**Figure 6:** (a) two different beam sequences intended to orientate the particle horizontally. Starting at the (blue) star with the particle aligned along the beam axis, switching directly to two radially displaced annular beams (orange dotted line), leads to the particle either escaping or aligning vertically in one of the beams. By adding a single intermediate potential the particle can be orientated horizontally (solid green line). (b) Simulated particle trajectory with one intermediate pattern between vertical and horizontal with a delay of 0.1s. Solid line shows simulation without Brownian motion, jagged gray line shows simulation with Brownian motion. Insets show digitally enhanced experimental images of an *E. coli* a short period after each transition.

Brownian motion. Our simulations showed that the time for the particle to reach equilibrium after each step was relatively short. Movie 2 shows an *E. coli* being orientated between horizontal and vertical with two different switching rates.

The method we described here is not specific to the use of annular beams to orientate particles. In this paper we choose to focus our attention on annular beams to create a more consistent narrative; however, we found that a similar result can be found using more Gaussian-like beams for particle orientation. The method for quantifying translation and rotation rates could be extended to other types of transitions; however, the method rapidly becomes more complex. For instance, reducing the step size below the time required for the particle to reach equilibrium makes each trajectory unique. In this case, the visualisation in figure 6 (b) becomes multi-dimensional and much harder to interpret. Adding rotational or translational degrees of freedom has a similar effect on increasing the dimensionality of the problem. The same orientation can be achieved by taking different trajectories through the translation/orientation hyperspace, each trajectory adding additional complexity to the problem. Instead of visualising the effect of each transition,  $\langle k \rangle$  could be used to create an objective function representing the quality of each trajectory. This would be useful for planning trajectories in complex light fields, or for classifying trajectories in fields inducing rotations or translations, such as for beams with orbital angular momentum. In particular, this approach could yield interesting results when using complex light fields to probe the change in a cell's visco-elastic properties in response to stimuli.

## 4. Summary

Optical tweezers are a useful tool for studying many different particle shapes including both spherical and non-spherical, as well as particles which are motile and non-motile. In order to study, for instance, how a bacterium swims at different heights above a surface, it is important to not just position these particles, but also orientate them. Non-motile particles can be orientated by dynamically varying the trap power; however, motile particles may escape if the power is lowered and the trap strength becomes too weak. By dynamically varying the potential, such as by using a spatial light modulator to change between discrete beam shapes, we can change the particle orientation. For *E. coli*, we demonstrated this technique by gradually rotating two annular traps, initially aligned along the beam axis, until finally aligned transverse to the beam axis. By simulating the particle and calculating the trap stiffness along the particle's trajectory, we determined that it should be feasible, and subsequently experimentally verified, that the particle orientation can be changed with a single intermediate step.

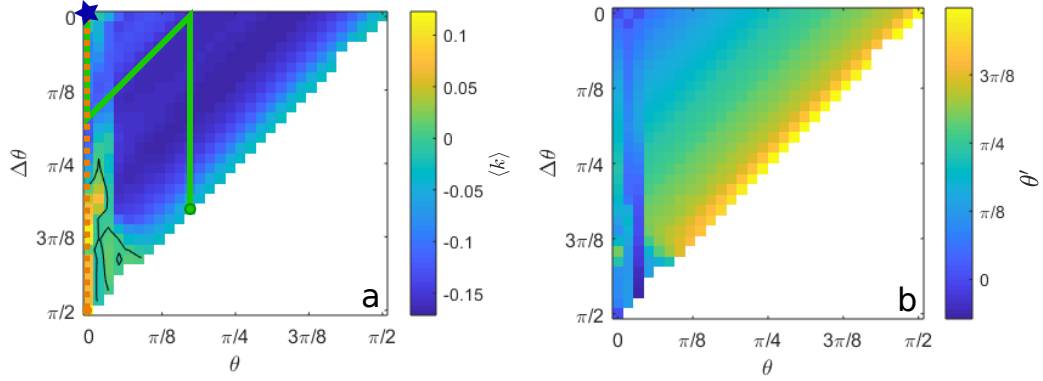


**Figure 7:** Rotational average trap stiffness and angle calculations for rod-shaped particle in an annular beam. (a) shows a graphical representation of the average trap stiffness towards the equilibrium  $\langle k \rangle$  (Eq. 7) for different step sizes ( $\Delta\theta$ ) from a given starting location ( $\theta$ ). The orange and green lines show the trajectory depicted in figure 6 (a). (b) shows the resulting particle angle after the step.

In our experiment we used annular beams. We were motivated to use annular beams as a possible method to improve angular trap strength for elongated particles, in a similar way as how annular beams improve axial trap strength for spherical particles. Using simulations, we explored how the inner radius of the annular beam affects the angular trap depth and trap stiffness. For high refractive rod-shaped particles, we noticed a significant improvement to the range of particles which could be trapped when using annular beams. However, for low refractive index particles, there was very little improvement. This suggested that for trapping of *E. coli* in water, annular beams wouldn't significantly improve trapping. However, for trapping higher contrast particles, such as elongated bacteria or viruses in air or vacuum, using an annular beam may be beneficial. We also explored adding spherical aberration to the beam. In some cases, the shape of the near-field intensity was less distorted with annular beams, leading to greater angular trap depth.

## Funding

This research was funded by the Australian Government through the Australian Research Council's Discovery Projects funding scheme (project DP180101002). Isaac Lenton acknowledges support from the Australian Government RTP Scholarship.

## Acknowledgements

We would like to thank Kate Peters, Steven Hancock, Minh-Duy Phan and Alvin Lo from the School of Chemistry and Molecular Biosciences at The University of Queensland for preparing the *E. coli* used in these experiments. We would also like to thank Shu Zhang for assisting with early experiments using scanned beams; and Carter Fairhall for his work testing different holographic optical traps.

## A. Trajectory average stiffness plots

Figure 7 was used to choose the trajectories shown in figure 6. Figure 7 (a) shows the stability of different steps with respect to the desired final orientation. For this case, the desired final orientation was  $\pi/2$  radians with respect to the beam axis. The figure shows each possible beam step size  $\Delta\theta$  for the initial orientations  $\theta$  between angles 0 and  $\pi/2$  radians. Figure 7 (b) shows the corresponding angle after each step. These figures suggest that once the particle has rotated past  $\approx \pi/8$  radians, any further rotation of the beams will lead to the particle moving towards the desired orientation.

In order to rotate the particle past the  $\pi/8$  angle, an initial step or steps need to be chosen. Figure 7 (a) shows that initial steps larger than approximately  $\pi/4$  radians result in an average tarp stiffness with the opposite sign. That is, the particle will not be attracted to the desired equilibrium. If we take a small step, the particle will orientate towards the

desired direction, however the range of good choices for subsequent steps reduces (i.e., the range of positive  $\langle k \rangle$  values becomes larger). By choosing a step larger than  $\pi/8$  radians but less than the unstable region, we can ensure that the next step is able to orientate the particle in the desired direction.

This particular configuration resulted in the particle angle after a stable step being equal to the particle angle with many infinitesimally small steps ( $\Delta\theta = 0$  line in figure 7 (b)). It is conceivable that there may be some situations where the particle angle after a transition doesn't match the infinitesimally small step case. In these cases, it might be more helpful to plot the difference between the resulting particle angle and the target (infinitesimally small step) angle instead of figure 7 (b). It may be necessary to generate multiple versions of these plots for each case where the angles don't match, or to generate a 3-dimensional plot for  $\langle k \rangle$  and  $\theta'$  with all combinations of  $\theta$ ,  $\Delta\theta$  and initial particle orientation. Alternatively, it may be easier to simply avoid such cases and only choose transitions which lead to the particle having the same orientation as the infinitesimally small step case.

## CRediT authorship contribution statement

**Isaac C. D. Lenton:** Software, Investigation, Writing - Original Draft. **Declan J. Armstrong:** Investigation. **Alexander B. Stilgoe:** Writing - Review & Editing, Supervision. **Timo A. Nieminen:** Funding Acquisition, Writing - Review & Editing, Supervision. **Halina Rubinsztein-Dunlop:** Funding Acquisition, Writing - Review & Editing, Supervision.

## References

- Ashkin, A., 1970. Acceleration and Trapping of Particles by Radiation Pressure. *Phys. Rev. Lett.* 24, 156–159. doi:10.1103/PhysRevLett.24.156.
- Ashkin, A., 1992. Forces of a single-beam gradient laser trap on a dielectric sphere in the ray optics regime. *Biophys. J.* 61, 569–582. doi:10.1016/S0006-3495(92)81860-X.
- Ashkin, A., Dziedzic, J., 1987. Optical trapping and manipulation of viruses and bacteria. *Science* 235, 1517–1520. doi:10.1126/science.3547653.
- Ashkin, A., Dziedzic, J.M., 1971. Optical Levitation by Radiation Pressure. *Appl. Phys. Lett.* 19, 283–285. doi:10.1063/1.1653919.
- Ashkin, A., Dziedzic, J.M., Bjorkholm, J.E., Chu, S., 1986. Observation of a single-beam gradient force optical trap for dielectric particles. *Opt. Lett.* 11, 288–290. doi:10.1364/OL.11.000288.
- Berg, H.C., 2004. *E. coli in Motion*. Springer-Verlag New York. doi:10.1007/978-0-387-21638-6.
- Bui, A.A.M., Kashchuk, A.V., Balanant, M.A., Nieminen, T.A., Rubinsztein-Dunlop, H., Stilgoe, A.B., 2018. Calibration of force detection for arbitrarily shaped particles in optical tweezers. *Sci. Rep.* 8, 1–12. doi:10.1038/s41598-018-28876-y.
- Bütaitė, U.G., Gibson, G.M., Ho, Y.L.D., Taverne, M., Taylor, J.M., Phillips, D.B., 2019. Indirect optical trapping using light driven micro-rotors for reconfigurable hydrodynamic manipulation. *Nat. Commun.* 10, 1215. doi:10.1038/s41467-019-08968-7.
- Cao, Y., Stilgoe, A.B., Chen, L., Nieminen, T.A., Rubinsztein-Dunlop, H., 2012. Equilibrium orientations and positions of non-spherical particles in optical traps. *Opt. Express* 20, 12987–12996. doi:10.1364/OE.20.012987.
- Carmon, G., Feingold, M., 2011. Rotation of single bacterial cells relative to the optical axis using optical tweezers. *Opt. Lett.* 36, 40–42. doi:10.1364/OL.36.000040.
- Català, F., Marsà, F., Montes-Usategui, M., Farré, A., Martín-Badosa, E., 2017. Extending calibration-free force measurements to optically-trapped rod-shaped samples. *Sci. Rep.* 7, 42960. doi:10.1038/srep42960.
- Dear, R.D., Burnham, D.R., Summers, M.D., McGloin, D., Ritchie, G.A.D., 2012. Single aerosol trapping with an annular beam: improved particle localisation. *PCCP* 14, 15826–15831. doi:10.1039/C2CP42925J.
- Dholakia, K., Čížmár, T., 2011. Shaping the future of manipulation. *Nat. Photonics* 5, 335. doi:10.1038/nphoton.2011.80.
- Favre-Bulle, I.A., Stilgoe, A.B., Rubinsztein-Dunlop, H., Scott, E.K., 2017. Optical trapping of otoliths drives vestibular behaviours in larval zebrafish. *Nat. Commun.* 8, 1–7. doi:10.1038/s41467-017-00713-2.
- Gauthier, G., Lenton, I., Parry, N.M., Baker, M., Davis, M.J., Rubinsztein-Dunlop, H., Neely, T.W., 2016. Direct imaging of a digital-micromirror device for configurable microscopic optical potentials. *Optica* 3, 1136–1143. doi:10.1364/OPTICA.3.001136.
- Gerchberg, R.W., Saxton, W.O., 1971. A practical algorithm for the determination of phase from image and diffraction plane pictures. *Optik* 35, 237–250.
- Hörner, F., Woerdemann, M., Müller, S., Maier, B., Denz, C., 2010. Full 3D translational and rotational optical control of multiple rod-shaped bacteria. *J. Biophotonics* 3, 468–475. doi:10.1002/jbio.201000033.
- Huang, J., Liu, X., Zhang, Y., Li, B., 2015. Optical trapping and orientation of Escherichia coli cells using two tapered fiber probes. *Photonics Res.* 3, 308–312. doi:10.1364/PRJ.3.000308.
- Itoh, H., Matsumoto, N., Inoue, T., 2009. Spherical aberration correction suitable for a wavefront controller. *Opt. Express* 17, 14367–14373. doi:10.1364/OE.17.014367.
- Kashchuk, A.V., Nieminen, T.A., Rubinsztein-Dunlop, H., Stilgoe, A.B., 2019. High-speed transverse and axial optical force measurements using amplitude filter masks. *Opt. Express* 27, 10034–10049. doi:10.1364/OE.27.010034.
- Lamstein, J., Bezryadina, A., Preece, D., Chen, J.C., Chen, Z., 2017. Optical tug-of-war tweezers: shaping light for dynamic control of bac-

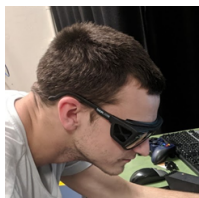


- terial cells (Invited Paper). Chin. Opt. Lett., COL 15, 030010. URL: <https://www.osapublishing.org/col/abstract.cfm?uri=col-15-3-030010>.
- Lang, M.J., Fordyce, P.M., Engh, A.M., Neuman, K.C., Block, S.M., 2004. Simultaneous, coincident optical trapping and single-molecule fluorescence. Nat. Methods 1, 133–139. doi:10.1038/nmeth714.
- Lei, M., Li, Z., Yan, S., Yao, B., Dan, D., Qi, Y., Qian, J., Yang, Y., Gao, P., Ye, T., 2013. Long-Distance Axial Trapping with Focused Annular Laser Beams. PLoS One 8, e57984. doi:10.1371/journal.pone.0057984.
- Lenton, I., Stilgoe, A.B., Nieminen, T.A., Loke, V.L.Y., Hu, Y., Knöner, G., Branczyk, A.M., Heckenberg, N.R., Rubinsztein-Dunlop, H., 2019. Optical Tweezers Toolbox. Zenodo doi:10.5281/zenodo.3352437.
- Meissner, R., Oliver, N., Denz, C., 2018. Optical Force Sensing with Cylindrical Microcontainers. Part. Part. Syst. Character. 35, 1800062. doi:10.1002/ppsc.201800062.
- Neuman, K.C., Block, S.M., 2004. Optical trapping. Rev. Sci. Instrum. 75, 2787–2809. doi:10.1063/1.1785844.
- Nieminen, T.A., Du Preez-Wilkinson, N., Stilgoe, A.B., Loke, V.L.Y., Bui, A.A.M., Rubinsztein-Dunlop, H., 2014. Optical tweezers: Theory and modelling. J. Quant. Spectrosc. Radiat. Transfer 146, 59–80. doi:10.1016/j.jqsrt.2014.04.003.
- Nieminen, T.A., Loke, V.L.Y., Stilgoe, A.B., Knöner, G., Branczyk, A.M., Heckenberg, N.R., Rubinsztein-Dunlop, H., 2007. Optical tweezers computational toolbox. J. Opt. A: Pure Appl. Opt. 9, S196–S203. doi:10.1088/1464-4258/9/8/s12.
- Nieminen, T.A., Rubinsztein-Dunlop, H., Heckenberg, N.R., 2003. Multipole expansion of strongly focussed laser beams. J. Quant. Spectrosc. Radiat. Transfer 79-80, 1005–1017. doi:10.1016/S0022-4073(02)00335-7.
- Oliveira, L., Campos, W.H., Rocha, M.S., 2018. Optical Trapping and Manipulation of Superparamagnetic Beads Using Annular-Shaped Beams. Methods Protoc. 1, 44. doi:10.3390/mps1040044.
- Padgett, M., Bowman, R., 2011. Tweezers with a twist. Nat. Photonics 5, 343. doi:10.1038/nphoton.2011.81.
- Pan, Y.L., Berg, M.J., Zhang, S.S.M., Noh, H., Cao, H., Chang, R.K., Videen, G., 2011. Measurement and autocorrelation analysis of two-dimensional light-scattering patterns from living cells for label-free classification. Cytometry 79A, 284–292. doi:10.1002/cyto.a.21036.
- Roichman, Y., Grier, D.G., 2006. Projecting extended optical traps with shape-phase holography. Opt. Lett. 31, 1675–1677. doi:10.1364/OL.31.001675.
- Simpson, S.H., Hanna, S., 2011. Computational study of the optical trapping of ellipsoidal particles. Phys. Rev. A 84, 053808. doi:10.1103/PhysRevA.84.053808.
- Stilgoe, A.B., Heckenberg, N.R., Nieminen, T.A., Rubinsztein-Dunlop, H., 2011. Phase-Transition-like Properties of Double-Beam Optical Tweezers. Phys. Rev. Lett. 107, 248101. doi:10.1103/PhysRevLett.107.248101.
- Stilgoe, A.B., Kashchuk, A.V., Preece, D., Rubinsztein-Dunlop, H., 2016. An interpretation and guide to single-pass beam shaping methods using SLMs and DMDs. J. Opt. 18, 065609. doi:10.1088/2040-8978/18/6/065609.
- Stuart, D., Kuhn, A., 2018. Single-atom trapping and transport in DMD-controlled optical tweezers. New J. Phys. 20, 023013. doi:10.1088/1367-2630/aaa634.
- Volpe, G., Volpe, G., 2013. Simulation of a Brownian particle in an optical trap. Am. J. Phys 81, 224. doi:10.1119/1.4772632.
- Woerdemann, M., Alpmann, C., Esseling, M., Denz, C., 2013. Advanced optical trapping by complex beam shaping. Laser Photonics Rev. 7, 839–854. doi:10.1002/lpor.201200058.
- Wong, D.W.K., Chen, G., 2008. Redistribution of the zero order by the use of a phase checkerboard pattern in computer generated holograms. Appl. Opt. 47, 602–610. doi:10.1364/AO.47.000602.
- Wulff, K.D., Cole, D.G., Clark, R.L., DiLeonardo, R., Leach, J., Cooper, J., Gibson, G., Padgett, M.J., 2006. Aberration correction in holographic optical tweezers. Opt. Express 14, 4169–4174. doi:10.1364/OE.14.004169.
- Zhang, H., Liu, K.K., 2008. Optical tweezers for single cells. J. R. Soc. Interface doi:10.1098/rsif.2008.0052.

## Orientation of Swimming Cells with Annular Beams



Isaac Lenton is a PhD student under the supervision of Timo Nieminen, Alex Stilgoe and Halina Rubinsztein-Dunlop. His PhD topic is on theory, modelling and control of optical tweezers, with a focus on studying motile organisms using optical tweezers. However, he is also working on a range of other projects tangentially related to his PhD topic including light shaping, imaging using spatial light modulators, machine learning, and fabrication of micro-fluidic devices.



Declan Armstrong is a PhD student working under the supervision of Halina Rubinsztein-Dunlop. His PhD topic is focused on modelling and testing theories of biohydrodynamics, with particular focus on the study of cells under propulsion. Further areas of interest expand to studying the behaviour and control of optically trapped biological cells, and particles undergoing stochastic motion.



Dr Alexander Stilgoe received his PhD from The University of Queensland in 2012. His recent work has been focused on understanding light scattering for applications to imaging and force measurement and the dynamics and interactions of particles and molecules on the microscopic and nanoscopic scale. He has performed a large amount of computational work and some experimental work on the interaction of complex electromagnetic fields with microscopic particles, e.g. multiple beams and structured light under different conditions.



Timo Nieminen obtained his PhD at The University of Queensland in 1996. His main research interests can be broadly classified as electromagnetic theory and computational electromagnetics. The main focus of this work is the theory and modelling of optical trapping, and the scattering of electromagnetic waves by particles. This work includes the development of the Optical Tweezers Toolbox, a freely available Matlab toolbox for the computational modelling of optical tweezers, which is available at <https://github.com/ilent2/ott>. Other interests include physics education, the history of physics and the physics of history, photonics, biological applications of optics, astrophysics, and the cross-disciplinary application of research methodology and tools.



Professor Halina Rubinsztein-Dunlop's research interests are in the fields of atom optics, laser micromanipulation, nano optics, quantum computing and biophotonics. She has long standing experience with lasers, linear and nonlinear high-resolution spectroscopy, laser micromanipulation, and atom cooling and trapping. She was one of the originators of the widely used laser enhanced ionisation spectroscopy technique and is well known for her recent work in laser micromanipulation. She has been also working (Nanotechnology Laboratory, Göteborg, Sweden) in the field of nano- and microfabrication in order to produce the microstructures needed for optically driven micromachines and tips for the scanning force microscopy with an optically trapped stylus.